

# Design of High Performance Wide Band Rotman Lens In X-Band

Alireza Bayat<sup>#\*1</sup>, Shayan Kajbaf Vala<sup>#2</sup>, Ashkan Soleimani<sup>#3</sup>

<sup>#</sup>Department of communication engineering

Imam Khomeini international university, Iran

**Abstract**—In this paper a Rotman lens consisting of 13 beamports and 10 array ports offers a phase shift from -50 degree to +50 degree with 7.5 degree step in X band is presented. The structure of lens has been simulated using MATLAB and optimized with help of Genetic Algorithm then results have been imported to CST Microwave Studio and simulated. For reducing phase error, path-lengths have been optimized using Advanced Design System (ADS). By this way the magnitude error of different frequency is limited within 3 dB.

**Keywords**—rotman lens; beamforming network; x-band; wide scanning.

## I. INTRODUCTION

Application of Rotman lens as a feed structure for phased array antennas particularly in military applications has been increased recently. Rotman lens is a cost effective RF beam-former network which provides simultaneous wide scanning. The Rotman lens has been implemented in waveguide, microstrip, stripline and using surface wave transmission lines [1]. Rotman lens applies path delay mechanism to form the desired phase front at the array input. The path-length design mechanism in the microwave lens is independent of frequency thus it is typically considered as true-time delay (TTD) device.

In 1950, Ruze introduced the concept and design equations for microwave lenses that can provide the capability of wide-angle electronic scanning of narrow multiple beam [2]. In 1963 first microstrip lens with parallel-plate was introduced by Rotman[3]. Many kinds of Rotman lens has been studied in the past decades, including printed Rotman lens [4-6], graded dielectric substrate Rotman lens [7], and SIW Rotman lens [8].

Rotman lens consists of beam ports (input ports), array ports (output ports), dummy ports, and the transmission line connected to them (Shown in Fig. 1) [9]. Dummy ports are necessary in order to reduce the side wall reflections as well as to increase the adjacent beam port isolations [10]. By increasing number of beam ports, 3dB beam width would decrease thus coverage the space improves but by doing so phase error will be increased. Minimizing the phase error level could be challenging. In this work phase error is minimized by Genetic Algorithm using MATLAB in first place then optimized by using ADS for obtaining the shape of transmission lines.

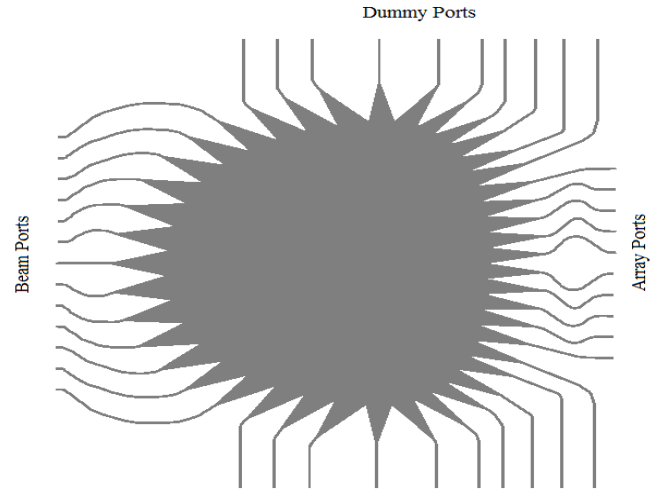


Fig.1 Schematic of Rotman lens

## II. THEORY AND DESIGN OF MICROSTRIP ROTMAN LENS

Geometry and design parameters of a microstrip Rotman lens is shown in Fig. 2 [11]. In this figure  $G, F_1$  and  $F_2$  are ideal focal and  $\epsilon_r, \epsilon_e, \epsilon_1$  are the permittivity of each regions.  $W$  is length of transmission line. Locus of beam ports is beam contour and locus of array ports is inner receiver contour. By using Rotman and Turner's method the equations of microstrip Rotman lens can be derived as follows [12]

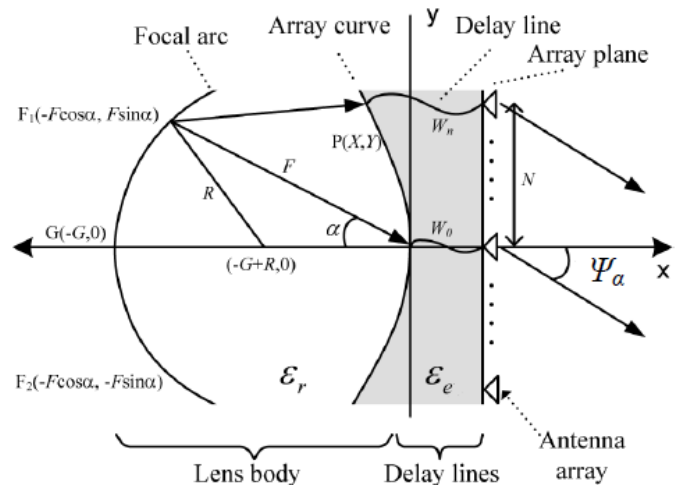


Fig.2 Geometry and design parameters of a Microstrip Rotman lens

$$F_1 P \sqrt{\epsilon_r} + W_n \sqrt{\epsilon_e} + N \sqrt{\epsilon_i} \sin(\psi_a) = F \sqrt{\epsilon_r} + W_0 \sqrt{\epsilon_e} \quad (1)$$

$$F_2 P \sqrt{\epsilon_r} + W_n \sqrt{\epsilon_e} - N \sqrt{\epsilon_i} \sin(\psi_a) = F \sqrt{\epsilon_r} + W_0 \sqrt{\epsilon_e} \quad (2)$$

$$GP \sqrt{\epsilon_r} + W_n \sqrt{\epsilon_e} = G \sqrt{\epsilon_r} + W_0 \quad (3)$$

From Fig. 2 we know the following equations hold true for locus of inner receiver.

$$(GP)^2 = (G + X)^2 + Y^2 \quad (4)$$

$$(F_1 P)^2 = (-F \cos(\alpha) - X)^2 + (-F \sin(\alpha) + Y)^2 \quad (5)$$

$$(F_2 P)^2 = (-F \cos(\alpha) - X)^2 + (-F \sin(\alpha) - Y)^2 \quad (6)$$

Divide both sides of equations (1)-(3) by  $G \sqrt{\epsilon_r}$  and the equations change into

$$\frac{F}{G} - \frac{W - W_0 \sqrt{\epsilon_e}}{G \sqrt{\epsilon_r}} - \frac{N \sin \psi_a \sqrt{\epsilon_i}}{G \sqrt{\epsilon_r}} \quad (7)$$

$$\frac{F}{G} - \frac{W - W_0 \sqrt{\epsilon_e}}{G \sqrt{\epsilon_r}} + \frac{N \sin \psi_a \sqrt{\epsilon_i}}{G \sqrt{\epsilon_r}} \quad (8)$$

$$\frac{GP}{G} = 1 - \frac{W - W_0 \sqrt{\epsilon_e}}{G \sqrt{\epsilon_r}} \quad (9)$$

Let

$$w = \frac{W - W_0}{G}, \beta = \frac{F}{G}, \xi = \frac{D \sin(\psi_a)}{f_1 \sqrt{\epsilon_r}}, x = \frac{X}{G}, y = \frac{Y}{G}.$$

Square (7)-(9) and equate with (4)-(6). After obtained these equations, the simplified simultaneous equations are shown blow

$$W^2 \frac{\epsilon_e}{\epsilon_r} + \left(\frac{N \sin \psi_a}{G}\right)^2 \frac{\epsilon_i}{\epsilon_r} - 2\beta W \frac{\sqrt{\epsilon_e \epsilon_i}}{\epsilon_r} = x^2 + y^2 + 2\beta x \cos(\alpha) \quad (10)$$

$$\frac{\beta N \sin \psi_a \sqrt{\epsilon_i}}{G \sqrt{\epsilon_r}} - \frac{WN \sin \psi_a \sqrt{\epsilon_e \epsilon_i}}{G \epsilon_r} = \beta y \sin(\alpha) \quad (11)$$

$$2x + x^2 + y^2 = W^2 \frac{\epsilon_e}{\epsilon_r} - 2W \frac{\sqrt{\epsilon_e}}{\sqrt{\epsilon_r}} \quad (12)$$

Note we are looking for the locus of point P(X, Y), which actually forms the receiving element port

counter, x, y, and w are variables. Solving equations (10)-(12) lead us to finding x and y as follows

$$y = \xi \frac{\sqrt{\epsilon_i}}{\sqrt{\epsilon_r}} \left( 1 - \frac{W \sqrt{\epsilon_e}}{\beta \sqrt{\epsilon_r}} \right) \quad (13)$$

$$x = \frac{\epsilon_i N^2 \sin^2 \psi_a}{2\epsilon_r (\beta \cos \alpha - 1)} + \frac{(1 - \beta)W}{\beta \cos \alpha - 1} \sqrt{\frac{\epsilon_e}{\epsilon_r}} \quad (14)$$

w is formulated from (10)-(12) into an standard equation show in(13)

$$\frac{a\epsilon_r}{\epsilon_e} W^2 + b \sqrt{\frac{\epsilon_e}{\epsilon_r}} W + c = 0 \quad (15)$$

$$W = \frac{\sqrt{\epsilon_e} - b \pm \sqrt{b^2 - 4ac}}{\sqrt{\epsilon_r} 2a} \quad (16)$$

Where

$$a = 1 - \left(\frac{1 - \beta}{1 - \beta \cos \alpha}\right)^2 - \frac{\xi^2 \epsilon_i}{\beta^2 \epsilon_r} \quad (17)$$

$$b = -2 + \frac{2\xi^2 \epsilon_i}{\beta \epsilon_r} + 2 \left(\frac{1 - \beta}{1 - \beta \cos \alpha}\right) - \frac{\xi^2 \sin^2 \alpha (1 - \beta) \epsilon_i}{(1 - \beta \cos \alpha)^2 \epsilon_r} \quad (18)$$

$$c = \left( -\xi^2 + \frac{\xi^2 \sin^2 \alpha}{1 - \beta \cos \alpha} - \frac{\xi^2 \sin^4 \alpha}{4(1 - \beta \cos \alpha)} \right) \frac{\epsilon_i}{\epsilon_r} \quad (19)$$

Now with help of x, y and winner receiver contour and the transmission lines will be obtain.

These equations have been based on 3 focal but in fact more than 3 focal is needed. To determine their locations the beam contour has been assumed as acircular shape that has all the three focal points. Beam port coordinates are given as follows

$$y_b = -x_b \tan \theta \quad (20)$$

$$x_b = \frac{1}{2} \frac{a[-2a + 2ab + 2\sqrt{a^2 b^2 - b^2 \tan^2 \theta} + 2b^3 \tan^2 \theta]}{a^2 + b^2 \tan^2 \theta} \quad (21)$$

Where  $\theta$  is the beam subtended angle.

### III. SIMULATION AND OPTIMIZATION

After obtain the lens formula, for minimizing phase error as much as possible, a proper MATLAB code is used and optimized locus of beam contour is obtained. Results of MATLAB have been imported to CST Microwave Studio to draw shape of lens. Finally results of CST Microwave Studio have been imported to ADS and final shape of lens for obtaining least phase error are specified.

These simulations and optimizations will be discussed by details in following subsections.

#### A. Matlab simulation

By using equations(13)-(20) we designed a unique MATLAB code to produce coordinates of beam ports and array ports as shown in Fig. 3.

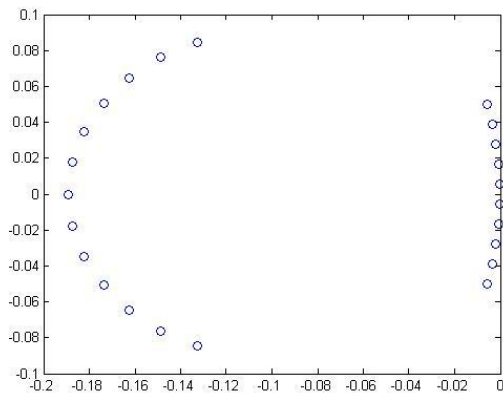


Fig. 3. Coordinates of beam ports and array ports

Many parameters affect the phase error but  $G/N$ ,  $\beta$  and  $\gamma$ , where  $\gamma$  is equal as follows

$$\gamma = \frac{\sin(\psi_a)}{\sin(\alpha)}$$

These parameters are optimized by Genetic Algorithm for reducing phase error as shown in Fig. 4.

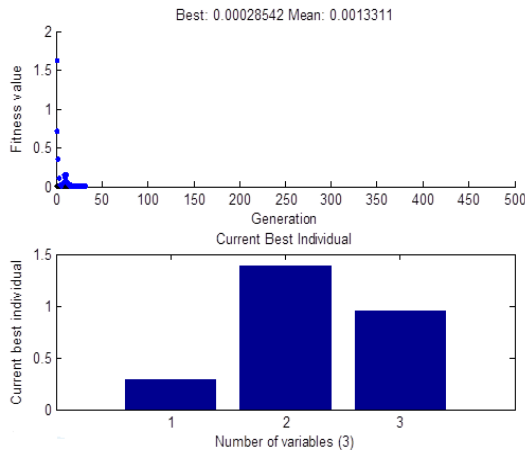


Fig. 4. Optimization of phase error by using MATLAB

#### B. CST Microwave Studionad ADS simulation

Results of MATLAB simulation imported to CST Microwave Studio to shape the lens. The model is constructed on Rogers 4003 substrate with permittivity of 3.55 and the thickness of 0.8 mm as shown in Fig. 5.

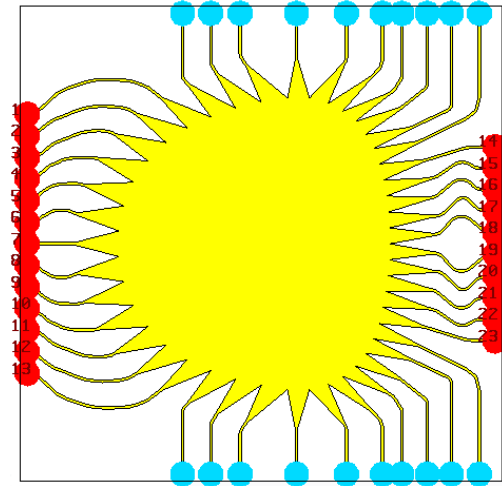


Fig. 5. Schematic of Rotman lens

Ports 1 to 13 are beam ports and ports 14 to 23 are array ports while other ports are dummy ports.

The final model of lens for optimizing shape of transmission lines is imported to ADS. By defining proper goals in ADS, best shape of transmission lines are obtained.

#### C. Analysis

The reflection and isolation characteristic of the beam ports and array ports of microstrip Rotman lens are measured and shown in Fig. 6 and Fig. 7.

(22)

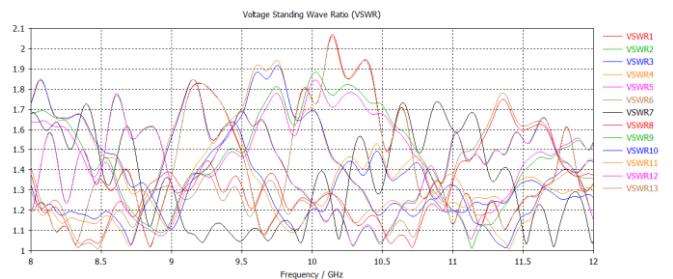


Fig. 6. VSWR parameters of beam ports of the lens

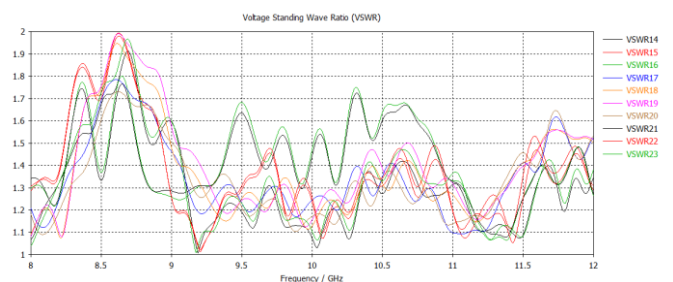


Fig. 7. VSWR parameters of array ports of the lens

S parameters of output ports (array ports) are shown in Fig. 8 to Fig. 13. Note that because of high number of input and output ports just 3 outputs and 3 inputs are shown.

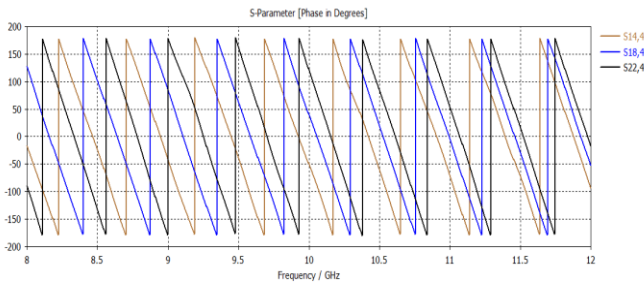


Fig.8 phase of s-parameters of port 4

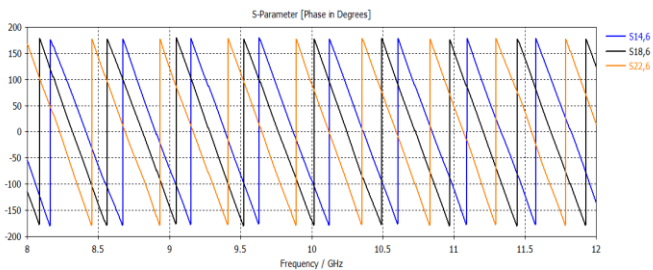


Fig.9 phase of s-parameters of port 6

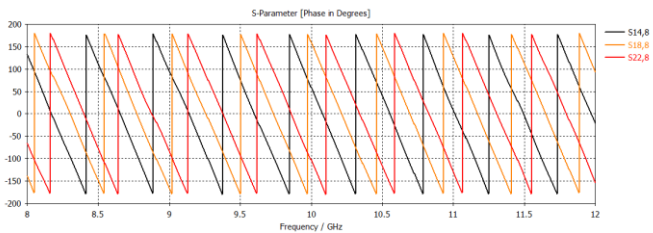


Fig.10 phase of s-parameters of port 8

As you can see in Fig.8 to Fig. 10, the phase of s-parameters is linear in X band frequency. It shows that a linear phase shift across the aperture is obtained so phase error is least. The magnitude of these s-parameters are shown in Fig. 11 to Fig. 13.

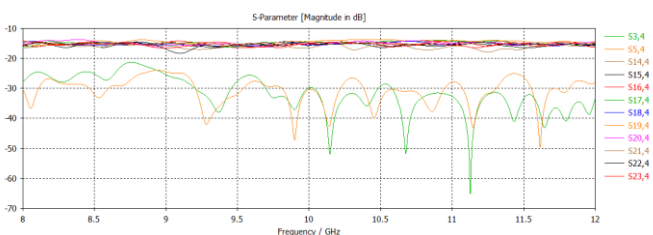


Fig.11 magnitude of s-parameters of port 4

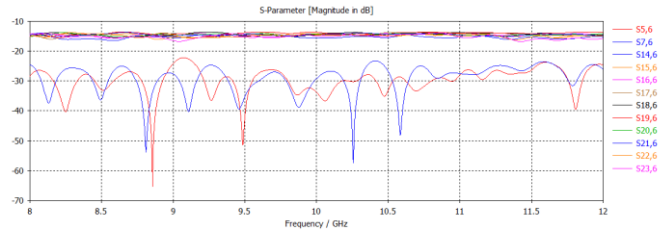


Fig.12 magnitude of s-parameters of port 6

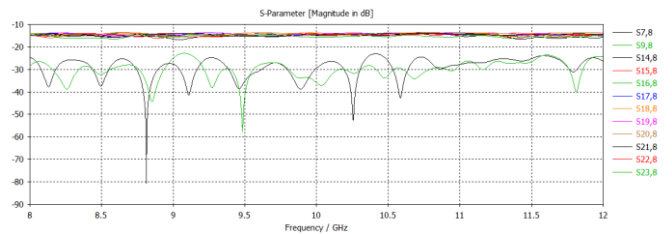


Fig.13 magnitude of s-parameters of port 8

As you can see in Fig. 11 to Fig.13, the received energy with fluctuation to output ports are below 3dB and the coupling effect is below -20dB. This feature indicates that an acceptable amplitude distribution is obtained and this lens can be applied to phase array antennas.

Fig. 14 shows electric field distribution on the lens if port 4 is excited. As you can see most of electric field propagates to output ports, backscattered waves are absorbed in dummy ports and coupling effect between input ports is nearly zero.

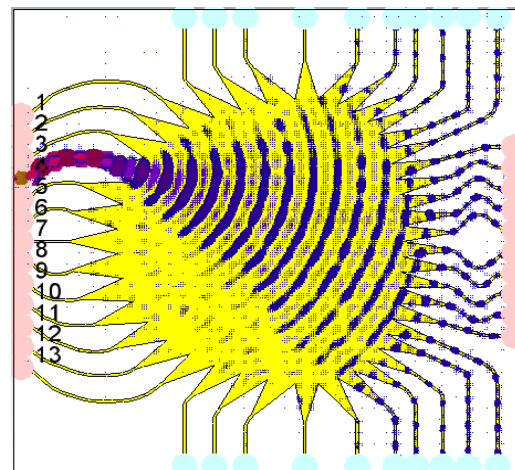


Fig. 14. Electric field distribution on lens

The normalized pattern of the lens is shown in Fig. 15. This figure shows that this lens has the ability to scan -50 degree to 50 degree with step of 7.5 degree.

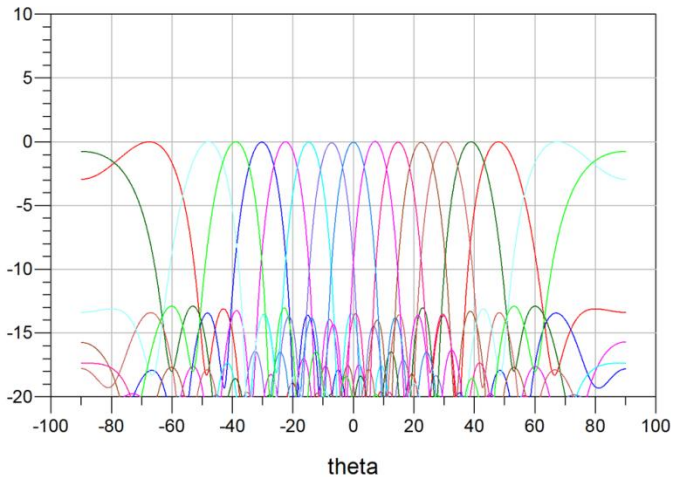


Fig. 13. Pattern of Rotman lens

#### IV. CONCLUSIONS

In this work, design formulations for microstrip Rotman lens was formed. The lens is designed on Rogers RT4003 substrate and can be applied for phase array antennas with ability to scan -50 degree to 50 degree with step of 7.5 degree.

The output characteristic of simulations indicates that the results fit perfectly well with theory in the x-band frequency.

#### REFERENCES

- [1] O. Kilic and S. Weiss, "Dielectric Rotman Lens Design For Multi-Function RF Antenna Application," *IEEE APS Symp.*, June 2004.
- [2] J. Ruze, Wide angle metal plate optics, *proc IRE* 38 (1950), 53-59.
- [3] W. Rotman and R.F. Tuner, Wide-angle microwave lens for line source application, *IEEE trans antenna Propag* AP-11 (1963), 623-632.
- [4] Musa, L. ;Smith, MS., Microstrip port design and sidewall absorption for printed Rotman lenses, *Microwave, Antennas and Propagation*, *IEEE Proceedings H*, Vol.136, No.1, Feb 1989, pp.53-58.
- [5] Carlegrim, Borje, Pettersson, Lars, Rotman lens in microstrip technology, *Microwave Conference*, 1992. 22<sup>nd</sup> European, 5-9 Sept. 1992, pp. 882-887.
- [6] Kim, J., Cho, C.S., Barnes, F.S., Dielectric Slab Rotman Lens for Microwave/Millimeter Wave Applications, *IEEE Transactions on Microwave Theory and Techniques*, Vol.53, No.8 Aug. 2005, pp.2622-2627.
- [7] Schulwitz, L., Mortazawi, A., A New Low Loss Rotman Lens Design Using a Graded Dielectric Substrate, *IEEE Transactions on Microwave Theory and Techniques*, Vo. 56, No. 12, Dec. 2008, pp. 2734-2741.
- [8] Yu Jian Cheng, Wei Hong, KeWu, Zhen Qi Kuai, etc., Substrate Integrated Waveguide (SIW) Rotman Lens and Its Ka-Band Multibeam Array Antenna Applications, *IEEE Transactions on Antennas and Propagation*, Vol. 56, No. 8, Aug. 2008, pp. 2504-2513.
- [9] Archer D. H, Maybell M. J, Rotman lens Development history at Raytheon Electric Warfare Systems 1967-1995, *Antennas and Propagation Society International Symposium*.
- [10] J. Dong, H.-C. Ou, A. I. Zaghoul, "Measurement Investigation of Microstrip Lens Sidewall's Termination," in *USNC/URSI National Radio Science Meeting South Carolina*, 2009.
- [11] Woosung Lee, Jaeheung Kim, Young Joong Yoon, Compact Two-Layer Rotman Lens-Fed Microstrip Antenna Array at 24 GHz, *IEEE Transactions on Antennas and Propagation*, Vol. 59, No. 2, February 2011, pp. 460-466.
- [12] Dong J ,Zaghoul A I, Rotman R ,Phase-error performance of multi-focal and non-focal two-dimensional Rotman lens designs, *Microwaves, Antennas & Propagation IET*, Vol.4, pp. 2097-2103 ,2010